A ONE-DIMENSIONAL HYDRO-SEDIMENT-MORPHODYNAMIC MODEL FOR THE CHANGJIANG WATERWAY

CHUNCHEN XIA
School of Civil Engineering and Architecture, Zhejiang University of Technology, Hangzhou, China. e-mail: xiacc@zjut.edu.cn.

HUI LIANG
State Key Laboratory of Water Resources and Hydropower Engineering Science, Wuhan University, Wuhan, China., e-mail: 744190927@qq.com.

ZHIXIAN CAO
State Key Laboratory of Water Resources and Hydropower Engineering Science, Wuhan University, Wuhan, China., e-mail: zxcao@whu.edu.cn.

SONGBAI PENG
Changjiang Waterway Institute of Planning and Design, Wuhan, China., e-mail: 13908628610@139.com.

YOUWEI LI
Changjiang Waterway Institute of Planning and Design, Wuhan, China., e-mail: 9057784@qq.com.

QIFENG LIU
Changjiang Waterway Institute of Planning and Design, Wuhan, China., e-mail: 309180864@qq.com.

WEI ZHANG
Changjiang Waterway Institute of Planning and Design, Wuhan, China., e-mail: 48774769@qq.com.

ABSTRACT

The Changjiang (Yangtze River) is one of the longest rivers in the world and plays a crucial role in waterborne freight in China. The waterway conditions in the middle and lower Yangtze River may not well meet the increasingly demanding requirements of cost-effective navigation in line with the rapid economic development in the region. Quantitative understanding of the water flow, sediment transport and bed evolution is essential for the regulation and maintenance of the waterway, especially since the Three-Gorges Reservoir was put into operation. One-dimensional (1D) modelling is one of the most viable approaches to enhancing the understanding of the hydro-sediment-morphodynamic processes. Yet previous 1D models are simplified, mostly based on rather crude assumptions (especially the quasi-steady flow assumption), of which the effects have so far remained insufficiently understood. Here, a physically-based 1D numerical model is presented, which explicitly incorporates the interactions between the flow, sediment transport and morphological evolution, and features a wide application in natural rivers with unsteady flows and non-uniform sediment transport. The governing equations are numerically solved using the shock-capturing finite volume method with the HLLC approximate Riemann solver for the flow equations and SLIC approximate Riemann solver for the sediment equation respectively. The model is benchmarked against a spectrum of test cases, and then applied to the reach from Yichang to Gong'an in the middle Changjiang Waterway. It shows that the model is able to successfully resolve the propagations of flow and sediment transport and reveals the influences of the discharge in Yichang on the water levels downstream. The present work facilitates a viable and promising approach to the understanding of the Changjiang Waterway, in support of its regulation and management.

Keywords: hydro-sediment-morphodynamic processes, 1D numerical model, shock-capturing finite volume method, waterway regulation and management

1. INTRODUCTION

The Changjiang (Yangtze River) is one of the longest rivers in the world and plays a crucial role in waterborne freight in China. Since the Three-Gorges Reservoir was put into operation, the dam has stored most of the coarse sediments arriving from the upstream catchment. At downstream, the mean sediment size becomes much finer and the river bed is scoured. Accordingly, the shift of the dominating branch, the instability of bars and the drop of the low water level worsen the navigational conditions of Changjiang Waterway, which may not well meet the increasingly demanding requirements of cost-effective navigation in line with the rapid economic development in the region,

especially in the middle and lower reaches. Thus, quantitative understanding of the water flow, sediment transport and bed evolution is essential for the regulation and maintenance of the waterway.

Significant efforts have been devoted to enhancing the understanding of the hydro-sediment-morphodynamic processes in Changjiang Waterway. The hydrometric stations along the waterway provide a series of valuable data for investigation. Some researches use the data analytical methods (Yuan et al, 2012; Hu et al., 2015), but they are divorced from physical processes of flow, sediment and riverbed. Physical models based on similarity criterion can directly reflect the flow movement, but they usually take a lot of time and money and target for the specific cases. Numerical simulations are key tools in predicting flow propagations under complicated conditions. While fully three-dimensional modelling may facilitate very detailed resolution of the flow phenomena, the excessively high computing cost makes it unrealistic to be applied to large-scale cases. Comparatively, one-dimensional (1D) shallow water hydro-sediment-morphodynamic (SHSM) models based on mass and momentum conservation feature a sensible balance between theoretical integrity and applicability and therefore have seen widespread applications in Changjiang modelling. Yet previous simplified 1D SHSM models are still widely used by engineers, mostly based on rather crude assumptions (especially the quasi-steady flow assumption), of which the effects remain insufficiently understood.

The finite volume method is one of the most promising approaches to solving the SHSM equations. The determination of the numerical flux is the key to this method in cases where the dependent variables may be steep-fronted or have discontinuous gradients and there are some available schemes to calculate the fluxes, for example, the Harten-Lax-van Leer (HLL) scheme, the HLLC scheme (a modified version of the HLL scheme), the Roe scheme and the slope limited centred (SLIC) scheme. In recent years, well-balanced schemes have been developed to improve the handling of irregular topographies (Qian et al., 2015) and the local time step method has been proposed to greatly decrease the computing cost (Hu et al., 2019).

This paper will present a complete1D SHSM model, which explicitly incorporates the interactions between the flow, sediment transport and morphological evolution, and features a wide application in natural rivers with unsteady flows and non-uniform sediment transport. The governing equations are numerically solved using the shock-capturing finite volume method combined with the HLL and SLIC approximate Riemann solvers. The model will be applied to the reach from Yichang to Gong'an in the middle Changjiang Waterway for calibration and validation, and it is also used in investigating the effects of upstream discharge on the downstream sections.

2. Mathematical Model

2.1 Governing equations

Under the framework of shallow water hydro-sediment-morphodynamics (Cao et al. 2017), the governing equations can be derived by directly applying the Reynolds Transport Theorem in fluid dynamics (Batchelor 1967, Xie 1990), or by integrating and averaging the three-dimensional mass and momentum conservation equations (Wu 2007). Consider longitudinally one-dimensional flow over a mobile and mild-sloped bed composed of non-cohesive sediments with N size classes (d_k denotes the diameter of the kth size sediment and k = 1, 2, …, N). The governing equations comprise the mass and momentum conservation equations for the water-sediment mixture flow, the size-specific mass conservation equations for the sediments, the mass conservation equations for the bed material (i.e. bed update equation), and the size-specific mass conservation equations for the sediment in active layer based on the widely used three-layer structure (i.e., bed load layer, active layer and substrate layer) (Hirano 1971).They can be written as

$$\frac{\partial A}{\partial t}+\frac{\partial Q}{\partial x}=\frac{E_T-D_T}{1-p}B+q_l \tag{1}$$

$$\frac{\partial (Q)}{\partial t}+\frac{\partial}{\partial x}\left(\frac{\beta Q^2}{A}\right)=-gA\frac{\partial (z_b+h)}{\partial x}-\frac{\tau_b}{\rho}-\frac{(\rho_s-\rho_w)}{\rho}\frac{Q}{A}\frac{B(E_T-D_T)(1-p-C)}{1-p} -\frac{(\rho_s-\rho_w)}{\rho}gAh_c\frac{\partial C}{\partial x}+\frac{\rho_l q_l u_l}{\rho}+\frac{(\rho_s-\rho_w)q_l}{\rho}\frac{Q}{A}(C-S) \tag{2}$$

$$\frac{\partial}{\partial t}(Ac_k)+\frac{\partial(\gamma_k Q c_k)}{\partial x}=(E_k-D_k)B+q_l s_k \tag{3}$$

$$\frac{\partial A_b}{\partial t}=\frac{(E_T-D_T)B}{1-p} \qquad \frac{\partial \delta f_{ak}}{\partial t}+f_{lk}\frac{\partial \xi}{\partial t}=\frac{D_k-E_k}{1-p} \tag{4,5}$$

where t = time; x = streamwise coordinate; A = cross-section area; h = flow depth; Q = flow discharge; B = channel width; g = gravitational acceleration; τ_b = bed friction; p = bed sediment porosity; β = momentum correction coefficient; h_c = water depth at centroid; γ_k = velocity discrepancy coefficient between the sediment and the mixture flow; c_k = depth-averaged size-specific volumetric sediment concentration and $C=\sum c_k$= total sediment concentration; E_k and D_k = sediment entrainment and deposition fluxes across the bottom boundary of flow, representing the sediment exchange between the water column and bed, $E_T=\sum E_k$ and

$D_T = \sum D_k$ are total sediment entrainment and deposition, respectively; A_b = cross-sectional area of the bed; z_b = bed elevation; ρ = density of water-sediment mixture flow; ρ_w and ρ_s = densities of water and sediment. ρ_l = density of the tributaries; q_l = discharge of the tributaries per unit width; u_l = velocities of the tributaries; s_k = size-specific volumetric sediment concentration of the tributaries; δ = thickness of the active layer and $\delta = 2d_{84}$, where d_{84} is the particle size at which 84% of the sediment are finer; f_{ak} = fraction of the *k*th size sediment in the active layer; $\xi = z_b - \delta$ = elevation of the bottom surface of the active layer; and f_{lk} = fraction of the *k*th size sediment in the interface between the active layer and substrate layer.

Unlike some simplified models, the present model explicitly accommodates the physical processes and can be widely used in alluvial rivers. *First*, the present model uses *A* and *Q* as primary variables for flow (Eqs. (1)-(3)), which are different from the models with depth *h* and velocity *u* applied in engineering practice, so it can better describe the complex section shapes of natural channels. *Second*, different from the simplified models with the assumption of very slow bed evolution (Parker et al.1986), the present model is physically coupled, which explicitly incorporates the interactions between flow, sediment transport and bed evolution. The first term on the right hand side (RHS) of Eq. (1) represents the mass exchange between the flow and the erodible and the third term on the RHS of Eq. (2) shows the corresponding momentum transfer, which reflect the complete physical phenomena and can properly resolve the strong feedback impacts of bed deformation (e.g., dam-break flow over erodible bed (Cao et al. 2004)). *Third*, the non-capacity approach (Cao et al. 2012, 2016) involved in the present model is generally justified as opposed to the simplified capacity approach (Postacchini et al. 2014). The former determines sediment transport by incorporating the contributions of advection due to mean flow velocity and of the mass exchange with the bed (Eq. (3)), while the latter presumes the sediment concentration to be always equal to the transport capacity determined exclusively by the local flow and bed conditions, which are only conditionally applicable if sediment adaptation to capacity regime is fulfilled sufficiently rapidly and within an adequately short distance. *Fourth*, following the unsteady property of flow, the time derivatives in governing equations are all considered, instead of being ignored in quasi-steady flow models. On the basis of quasi-steady flow assumption (Li and Xie 1986), the computational period is divided into a number of time intervals, and during each time interval, the flow discharge is assumed to be constant and the flow is assumed to be steady. This practice is still widespread used by engineers maybe for its low computing cost, but one the one hand, it may evoke problems in terms of modeling accuracy, on the other hand, the reduced computing time may not necessarily have an edge with current fast-developing computing technology. *Moreover*, due to the ubiquitous non-uniform sediment in alluvial rivers, the sheltering/exposure effects on sediments of different sizes and the variation of bed sediment composition evaluated based on active layer proposed by Hirano are also included in the present model (Eqs. (4)-(5)). *In addition*, tributaries are needed to be considered. The second term on the RHS of Eq. (1), the last two terms on the RHS of Eq. (2) and the second term on the RHS of Eq. (3) reflect the mass and momentum effects by mixture flows and sediments of tributaries, respectively. In general, the present coupled model involves fewer assumptions, thereby minimizing the model uncertainty.

2.2 Model closure

Although the present model uses the fewer assumptions, the physical processes of sediment-laden flow in alluvial rivers are far from clear. So, a set of empirical relationships have to be introduced to close the governing equations, including the determination of the bed friction and momentum correction coefficient, sediment exchange fluxes, the velocity discrepancy coefficient between the sediment and the mixture flow and the fraction of the *k*th size sediment in the interface between the active layer and substrate layer.

The bed friction is determined by Manning's formula, which is

$$\tau_b = \rho g A n_0^2 u|u| / R^{4/3} \tag{6}$$

where R = the hydraulic radius; and n_0 = the Manning roughness, which can be obtained along with momentum coefficient β according to Cao et al. (2006). Based on the lateral velocity distribution, Cao et al. (2006) proposed the formula for overall roughness of a cross section and momentum correction coefficient, which reads,

$$\beta = \frac{AF}{Q^2} = \frac{I_1 I_{2R1}}{I_{R1}^{\ 2}} \qquad n_0 = \frac{I_{2R13}^{\ 1/2} I_1^{\ 7/6}}{I_{R1} P^{2/3}} \tag{7,8}$$

where P = wetted perimeter.

$$P = \int_{Bw} \sqrt{1+(\partial z_b/\partial y)^2}\, dy \qquad I_1 = \int_{Bw} (h'/h_m)\, dy \qquad I_{2R1} = \int_{Bw} (h'/h_m)^{2R+1} (n_m/n')^{3R}\, dy \tag{9,10,11}$$

$$I_{R1} = \int_{Bw} (h'/h_m)^{R+1} (n_m/n')^{3R/2}\, dy \qquad I_{2R13} = \int_{Bw} n'^2 (h'/h_m)^{2R-1/3} (n_m/n')^{3R} \sqrt{1+(\partial z_b/\partial y)^2}\, dy \tag{12,13}$$

where y = lateral coordinate, n' = local roughness at y, h' = flow depth at y, and n_m, h_m are the flow depth, and roughness at a reference location $y = y_m$. Generally, h_m can be defined as the maximum flow depth in a cross section, where the bed elevation is z_b, and n_m can be obtained by calibration.

The velocity discrepancy coefficient γ_k is estimated by the relation due to Greimann et al.(2008)

$$\gamma_k = \frac{u_*}{u}\frac{1.1\left(\theta_k / 0.047\right)^{0.17}\left(1-\exp\left(-5\theta_k / 0.047\right)\right)}{\sqrt{0.047}} \tag{14}$$

where u_* = bed shear velocity; u = average velocity; $\theta_k = u_*^2 / sgd_k$ =size-specific shields parameter with the specific gravity of sediment $s=(\rho_s-\rho_w)/\rho_w$. Generally, bedload sediment is usually transported at a velocity lower than the flow, i.e., γ_k <1. However, for suspended sediment, the value of γ_k can simply set equal to unity as the suspended sediment transport has nearly the same mean velocity as the flow.

Sediment entrainment due to fluctuations and sediment deposition by gravitational action are two distinct mechanisms involved in mass exchange with the bed, which are still poorly understood. Generally, the deposition flux can be computed by the local near-bed sediment concentration and the hindered settling velocity. And the entrainment flux is mostly based on the assumption that entrainment always occurs at the same rate as it does under capacity regime. Empirically, the size-specific sediment entrainment and deposition fluxes are estimated as

$$E_k = \lambda_k c_{ek}\omega_k\left(1-\lambda_k c_{ek}\right)^{m_k},\ D_k = \lambda_k c_k \omega_k\left(1-\lambda_k c_k\right)^{m_k} \tag{15,16}$$

where ω_k = size-specific settling velocity computed by the formula of Zhang and Xie (1993); and λ_k = empirical parameter representing the difference between the near-bed sediment concentration and the depth-averaged sediment concentration. Physically, for suspended sediment λ_k = 1 is used, while $\lambda_k = h / h_{bk}$, for bedload sediment, and $h_{bk} = \max(9u_*^2 / sg, 2d_k)$ =the thickness of bedload layer. The hindered effects on sediment settling in deposition flux come from the water as well as the sediments of other size fractions. $m_k = 4.45R_{pk}^{-0.1}$, $R_{pk} = \omega_k d_k / \nu_\mu$, and ν_μ is the kinematic viscosity of water. The size-specific sediment concentration at capacity c_{ek} is calculated as

$$c_{ek} = F_k q_k / (hu) \tag{17}$$

where q_k = size-specific transport rate at capacity regime and the formula of Wu et al. (2000) is adopted. In the processes of the incipient motion and movement of non-uniform sediments, the coarse grains are easier to be entrained than their counterparts in uniform cases because they have higher exposure chance to flow, while fine grains are more difficult to be entrained as they are more likely to be sheltered by coarse grains, which is known as the hiding and exposure effect. Thus F_k is the areal exposure fraction of kth sediment on the bed surface given by Parker (1991)

$$F_k = \frac{f_{ak}/\sqrt{d_k}}{\sum\left(f_{ak}/\sqrt{d_k}\right)} \tag{18}$$

According to Wu et al. (2000), each sediment size is transported as bed load and suspended load at the same time. Therefore, sediment transport rate of kth sediment can be determined as

$$\frac{q_k}{\sigma\sqrt{(\rho_s/\rho_w-1)gd_k^3}} = 0.0053\left[\left(\frac{\tilde{n}}{n}\right)^{1.5}\frac{\tau_b'}{\tau_{ck}}-1\right]^{2.2} + 0.0000262\left[\left(\frac{\tau}{\tau_{ck}}-1\right)\frac{u}{\omega_k}\right]^{1.74} \tag{19}$$

where σ = modification coefficient; $\tilde{n} = d_{50}^{1/6} / 20$ = Manning roughness corresponding to the grain resistance; τ_b' = bed shear stress; τ = shear stress at channel cross-section; $\tau_{ck} = 0.03\eta_k(\rho_s-\rho_w)gd_k$ = size-specific critical shear stress, and η_k = hiding and exposure factor computed by Wu et al. (2000).

In order to solve the Eq. (5), an empirical relation to evaluate f_{Ik} is needed to be introduced (Hoey and Ferguson 1994).

$$f_{Ik} = \begin{cases} f_{sk} & \partial\xi/\partial t \le 0 \\ \phi C_k / C_T + (1-\phi) f_{ak} & \partial\xi/\partial t > 0 \end{cases} \tag{20}$$

where f_{sk} = fraction of the kth size sediment in the substrate layer; ϕ = empirical weighting parameter, and ϕ = 0.7 is used here.

2.3 Numerical algorithm

The full set of the governing equations can be written in a format as

$$\mathbf{D}\frac{\partial \mathbf{U}}{\partial t} + \frac{\partial \mathbf{F}(\mathbf{U})}{\partial x} = \mathbf{S}_b(\mathbf{U}) + \mathbf{S}_f(\mathbf{U}) + \mathbf{S}_0(\mathbf{U}) \tag{21}$$

$$\mathbf{D} = \begin{bmatrix} B & 0 & 0 \\ 0 & 1 & 0 \\ 0 & 0 & 1 \end{bmatrix} \quad \mathbf{U} = \begin{bmatrix} \eta \\ Q \\ Ac_k \end{bmatrix} \quad \mathbf{F} = \begin{bmatrix} Q \\ \beta Q^2 / A \\ \gamma_k Q c_k \end{bmatrix} \tag{22a,b,c}$$

$$\mathbf{S}_b(\mathbf{U}) = \begin{bmatrix} 0 \\ -gA\dfrac{\partial \eta}{\partial x} \\ 0 \end{bmatrix} \qquad \mathbf{S}_f = \begin{bmatrix} 0 \\ -\dfrac{\tau_b}{\rho} \\ 0 \end{bmatrix} \tag{22d,e}$$

$$\mathbf{S}_0 = \begin{bmatrix} q_l \\ -\dfrac{(\rho_s-\rho_w)}{\rho} gAh_c \dfrac{\partial C}{\partial x} - \dfrac{(\rho_s-\rho_w)}{\rho}\dfrac{Q}{A}\dfrac{B(E_T-D_T)(1-p-C)}{1-p} + \dfrac{\rho_l q_l u_l}{\rho} + \dfrac{(\rho_s-\rho_w)q_l}{\rho}\dfrac{Q}{A}(C-S) \\ (E_k-D_k)B + q_l s_k \end{bmatrix} \tag{22f}$$

where $\eta = z_b + h$ = water level. And the transformation of Eq. (1) helps to promote numerical stability in computing, especially in natural rivers with sharp changing cross-sections.

The set of governing equations is numerically solved synchronously using the shock-capturing finite volume method. An explicit finite volume discretization of Eq. (21) gives, (Toro, 2001; Qian et al., 2015),

$$\mathbf{U}_i^* = \mathbf{U}_i^j - \frac{\Delta t}{\Delta x}\mathbf{D}_i^{-1}\left(\mathbf{F}_{i+1/2} - \mathbf{F}_{i-1/2}\right) + \Delta t \mathbf{D}_i^{-1}\mathbf{S}_{bi}\ , \quad \mathbf{U}^{j+1} = \mathbf{U}^* + \Delta t \mathbf{D}^{-1}\left(\mathbf{S}_f + \mathbf{S}_0\right) \tag{23a,b}$$

where Δt = time step; Δx = spatial step; i = spatial node index; j = time node index; and $\mathbf{F}_{i+1/2}$ = inter-cell numerical flux at $x = x_{i+1/2}$ .The scheme is monotone and needs to satisfy the Courant-Friedrichs-Lewy (CFL) condition $\Delta t = C_r \Delta x / \lambda_{\max}$, where $\lambda_{\max}$ = the maximum celerity computed from the Jacobian matrix; and C_r = Courant number.

In order to facilitate mathematical manipulation, the HLL approximate Riemann solver is adopted for the flow equations (i.e., Eqs. (1)-(2)) and SLIC approximate Riemann solver (Toro, 2001) is used for the sediment equation (i.e., Eq. (3)). Meanwhile, Eqs. (4) and (5) are solved separately from Eqs. (1)-(3) as they are in essence ordinary different equations. Yet all variables are updated at each time step. It is physically justified due to the fact that bed deformation is solely determined by the local entrainment and deposition fluxes.

3. Numerical case study

Study area is from Yichang to Gong'an in the middle Changjiang Waterway with the length of 178. 543 km, as shown in Figure 1. Yichang to Zhicheng is a transition zone from the bedrock gorges to the flood plain, about 54 km long, with a tributary (Qingjiang) flowing into the main channel. And from Zhicheng to Gong'an, there are two main outlets (Songzikou and Taipingkou) for the flow to be diverted to Dongting Lake which plays a flood regulatory role in the middle reach of Changjiang Waterway. Two period time of unsteady flows are investigated. The first period is from 1st March to 1st August, 2018, during which the upstream inflow is rising and the model parameters for reference roughness and modification coefficient of sediment transport rate are calibrated. This calibrated model is then applied to the second period from 1st August, 2018 to 1st March, 2019 to test its accuracy. In order to gain insight into how much the change of inflow would impact the Zhijiang and Shashi sections during the low flow period, which is a concern to the waterway management, the propagation time and variation in water level are investigated by the present model.

The initial conditions are obtained by the steady flow under the initial discharge of Yichang. The boundary conditions are determined by inflow discharge of Yichang and downstream water level of Gong'an. The spatial step is 2231.8 m, thus there are 81 computational sections. The time steps are calculated by CFL condition and the Courant number is 0.5. Table 1 summaries the distances between the important sections and the upstream boundary (Yichang) along with the functions of each sections.

3.1 Calibration: from 01/03/2018 to 01/08/2018

Because of the weak alluviation in the middle and lower reaches of Changjiang Waterway, the feedback of bed evolution has the limit effect on the flow. The roughness can be calibrated first by fixed bed case and then the mobile bed case is used to determine the modification coefficient of sediment transport rate. It can be easily understood that the relationship between roughness and water level is not monotonous for unsteady flow for a cross-section as it may be influenced by rising and falling of flows as well as channel regulation structures. Based on the measured data from hydrometric stations, the fitted roughness relationships (power functions) are used for different reaches of study area, as shown in Table 2. Figures 2 and 3 show the comparison between computed water level and the measured. It can be seen that computed water elevation agrees well with the measured in Shashi and Dengjiatai, most of the time the differences between the computed and measured are within 0.1 m. It is noted that the model simulates the unsteady flow process, which is different from traditional quasi-steady flow to separate the unsteady flow into several time intervals with constant discharge (i.e., steady flow). Figure 4 is the computed discharge of Zhicheng and Shashi sections compared with the measured data, which are in a good agreement. In our study, the tributaries mainly have an impact on the discharge in flood season, during which the Songzikou and Taipingkou help to release flood flows. So in Figure 4, there are little discrepancies between the computed results with or without tributary in Zhicheng as this section is at the

upstream of the outlets, whereas the differences are obvious for Shashi that the simulated discharge without considering tributary will significantly larger than the reality at the flood period (red and blue lines in Figure 4).

Combined with the calibrated roughness as shown in Table 2, the bed deformation due to sediment entrainment and deposition is incorporated into the model. The modification coefficient σ of sediment transport rate in Eq. (19) is 0.05. Figure 5 illustrates the good agreement of computed sediment concentration with the measured, in line with time of flood peak (Figure 4). The computed and measured bed elevation are shown in Figure 6. Generally, the computed and measured bed elevation have similar trend.

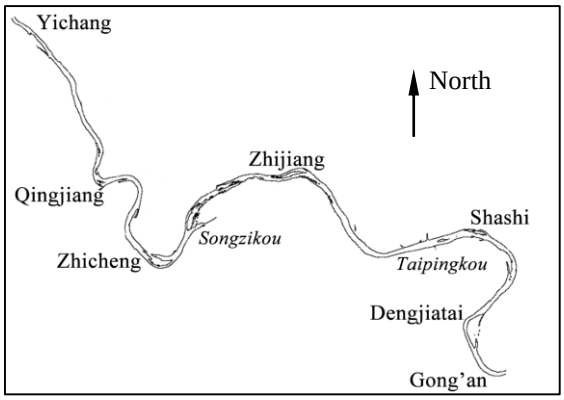

Figure 1. Sketch of study area

Table 1. Summary of important sections.

Sections	*x (km)*	*Notes*
Yichang	0	Upstream boundary
Qingjiang	35.352	Inflow Tributary
Zhicheng	54.705	Measured discharge/sediment
Songzikou	72.820	Outflow Tributary
Zhijiang	86.982	Study section
Taipingkou	133.095	Outflow Tributary
Shashi	145.988	Measured elevation/discharge/ sediment & Study section
Dengjiatai	157.393	Measured elevation
Gong'an	178.543	Downstream boundary

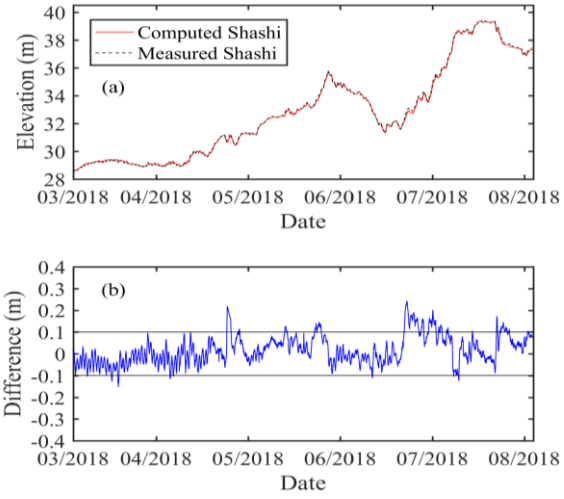

Figure 2. Water level of Shashi from 03/2018 to 08/2018

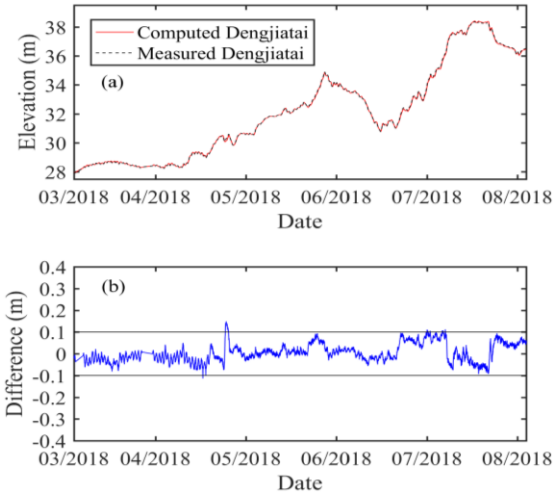

Figure 3. Water level of Dengjiatai from 03/2018 to 08/2018

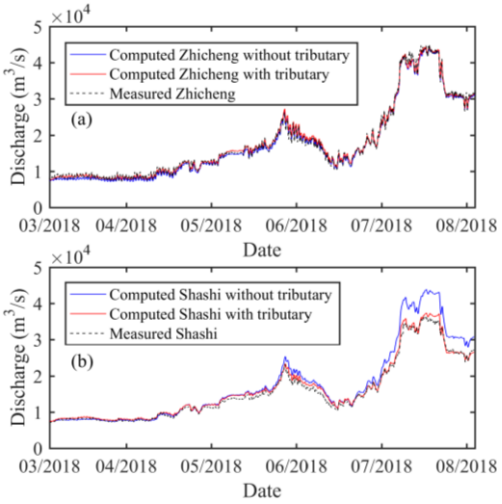

Figure 4. Discharge from 03/2018 to 08/2018

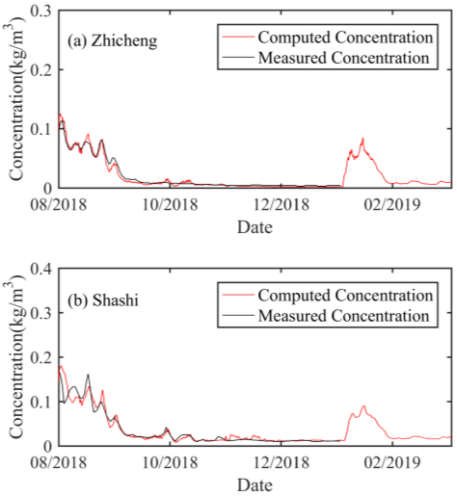

Figure 5. Sediment concentration from 03/2018 to 08/2018

3.2 Validation: from 01/08/2018 to 01/03/2019

This section uses calibrated roughness and modification coefficient to simulate the unsteady inflow from 01/08/2018 to 01/03/2019. Figures 7 and 8 show the computed water level in Shashi and Dengjiatai and the differences compared to the measured. Similar to the first period, the discrepancies are within 0.1 m in the

majority of the time. Figure 9 shows the sediment concentration of Zhicheng and Shashi sections, and the computed results agree with the measured. Figure 10 reflects the similar bed evolution trend as the measured. Thus, the good performance of the simulations underpins the ability of the present model to resolve the flow and sediment propagations and do further researches, in support of Changjiang management.

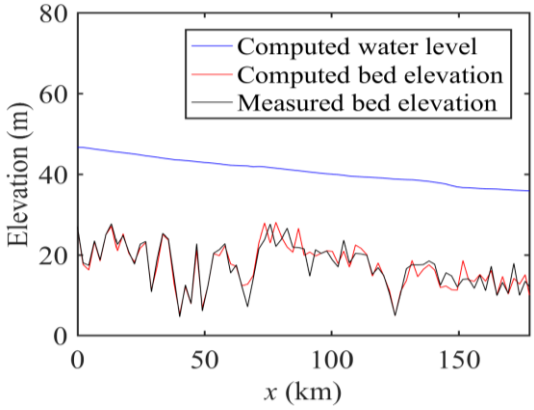

Figure 6. Bed elevation at 08/2018

Table 2. Roughness for different reaches

Reach	*Relation*
Yichang ~ Zhicheng	$n_m = -2E - 15Z^{7.2} + 0.035$
Zhicheng ~ Zhijiang	$n_m = -2E - 15Z^{7.2} + 0.0281$
Zhijiang ~ Taipingkou	$n_m = -2E - 15Z^{7.78} + 0.0343$
Taipingkou ~ Shashi	$n_m = -2E - 15Z^{7.2} + 0.039$
Shashi ~ Dengjiatai	$n_m = -2E - 15Z^{7} + 0.0217$
Dengjiatai ~ Gong'an	$n_m = -2E - 15Z^{7.73} + 0.022$

*Z is the water level

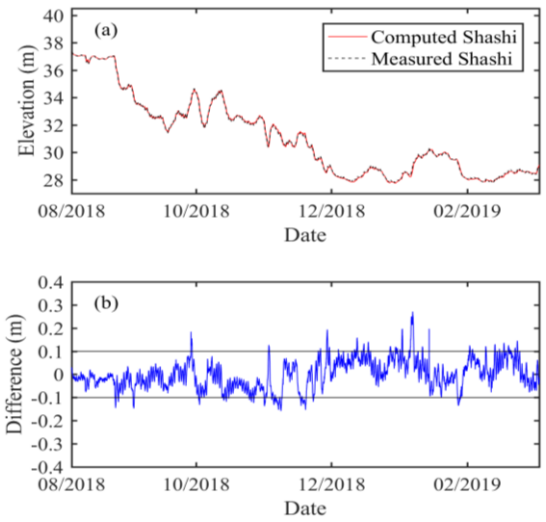

Figure 7. Water level of Shashi from 08/2018 to 03/2019

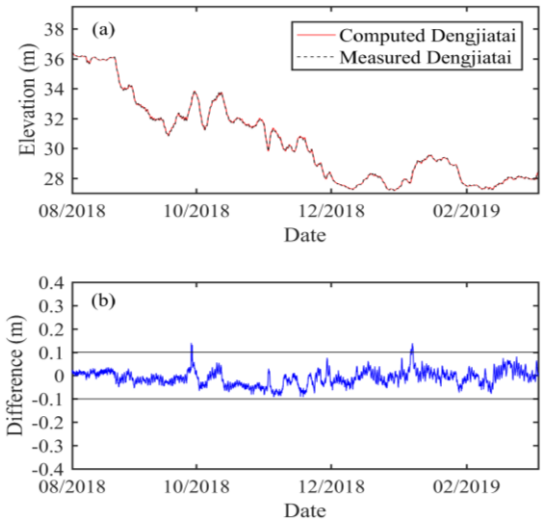

Figure 8. Water level of Dengjiatai from 08/2018 to 03/2019

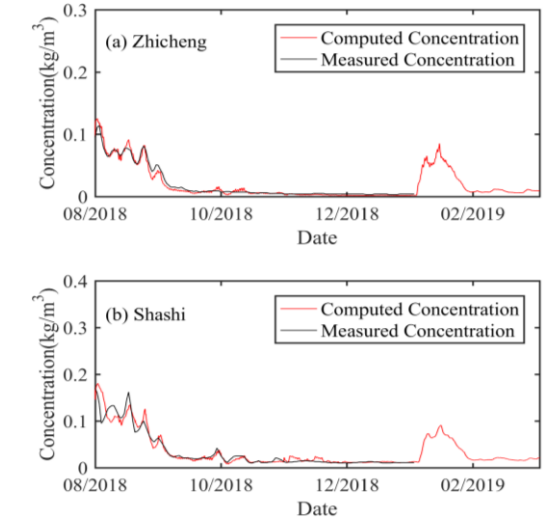

Figure 9. Sediment concentration from 08/2018 to 03/2019

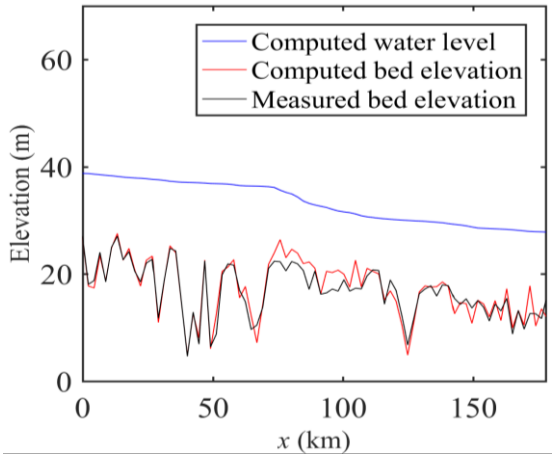

Figure 10. Bed elevation at 03/2019

3.3 Effects of upstream flows on Zhijiang and Shashi sections

Low flow period is important to waterway regulation and management. The increase or decrease of the inflow discharge will cause change in water level at downstream sections. Several study cases along with the simulated results are summarized in Table 3. The inflow rises or falls in 24 hours linearly. It can be seen from the table that the initial inflow discharge is larger, the time of propagation to the section is less for both rising and falling period. And for the same change degree of inflow discharge, affected time of falling water period is less than that of rising period. The change of water level is similar for both rising and falling processes. Because Yichang is closer than Shashi (Table 1), the flow front arrives at Zhijiang earlier than Shashi.

Table 3. Inflow influences on the Zhijiang and Shashi Sections

Study cases		Zhijiang		Shashi	
		Affect time (min)	Level change (m)	Affect time (min)	Level change (m)
Rising water in a day	6000~7000	362.6	0.678	659.8	0.941
	8000~10000	328.8	1.165	587.8	1.408
Falling water in a day	7000~6000	225.2	0.700	576.1	0.965
	10000~80000	181.0	1.156	444.3	1.347

4. CONCLUSIONS

A physically-based 1D numerical model is presented, which explicitly incorporates the interactions between the flow, sediment transport and morphological evolution and features wide applications in natural rivers with unsteady flows and non-uniform sediment transport. Solved by the shock-capturing finite volume method, the model is applied to study the reach from Yichang to Gong'an in the middle Changjiang Waterway. The performance of the model shows that it can successfully resolve the propagations of flow and sediment and reveals the influences of the discharge in Yichang on the water levels downstream. The present work facilitates a viable and promising approach to the understanding of the Changjiang Waterway, in support of its regulation and management.

ACKNOWLEDGMENTS

This research is supported by the Project of Changjiang Waterway Institute of Planning and Design.

REFERENCES

Batchelor, G. K. (1967). An Introduction to Fluid Dynamics, Cambridge University Press, England.

Cao, Z., Pender, G., Wallis, S., and Carling, P. (2004) Computational dam-break hydraulics over erodible sediment bed. *Journal of Hydraulic Engineering*, 130(7):689-703.

Cao, Z., Pender, G., Wallis, S., and Carling, P. (2006) Flow resistance and momentum flux in compound open channels. *Journal of Hydraulic Engineering*, 2006.132(11): 1272-1282.

Cao, Z., Li, Z., Pender, G., and Hu, P. (2012) Non-capacity or capacity model for fluvial sediment transport. *Water Management, Proceedings of Institution of Civil Engineers*, 165(4):193-211.

Cao, Z., Hu, P., Pender, G., and Liu, H. (2016) Non-capacity transport of non-uniform bed load sediment in alluvial rivers. *Journal of Mountain Science*, 13(3): 377-396.

Cao, Z., Xia, C., Pender, G., and Liu, Q. (2017) Shallow water hydro-sediment-morphodynamic equations for fluvial processes. *Journal of Hydraulic Engineering*, 143(5): 02517001.

Greimann, B., Lai, Y., and Huang, J. (2008). Two-dimensional total sediment load model equations. *Journal of Hydraulic Engineering*, 134(8):1142–1146.

Hirano, M. (1971) River bed degradation with armouring. *Proceedings of Japan Society of Civil Engineers*, Tokyo, Japan., pp. 55-65 (in Japanese).

Hoey, T., and Ferguson, R. (1994) Numerical simulation of downstream fining by selective transport in gravel bed rivers: Model development and illustration. *Water Resources Research* 30(7): 2251-2260.

Hu, C., Fang, C., and Cao, W. (2015) Shrinking of Dongting Lake and its weakening connection with the Yangtze River: Analysis of the impact on flooding. *International Journal of Sediment Research*, 30:256-262.

Hu, P., Lei, Y., Han, J., Cao, Z., Liu, H., and He, Z. (2019) Computationally efficient modeling of hydro-sediment-morphodynamic processes using a hybrid local time step/global maximum time step. *Advances in Water Resources*, 127:26-38.

Li, Y., and Xie, J. (1986). Mathematical modelling of two-dimensional flow in alluvial rivers. *Chin. J. Hydraul. Eng*., 11: 9-15 (in Chinese).

Parker, G., Fukushima, Y., and Pantin, H. M. (1986) Self-accelerating turbidity currents. *J Fluid Mech*, 171:145–81.

Parker, G. (1991) Selective sorting and abrasion of river gravel. I: Theory. *Journal of Hydraulic Engineering*. 117(2): 131-149.

Postacchini, M., Othman, I. K., Brocchini, M., and Baldock, T. E. (2014) Sediment transport and morphodynamics generated by a dam-break swash uprush: coupled vs uncoupled modelling. *Coastal Engineering*, 89:99-105.

Qian, H., Cao, Z., Pender, G., Liu, H., and Hu, P. (2015) Well-balanced numerical modelling of non-uniform sediment transport in alluvial rivers. *International Journal of Sediment Research*, 30(2): 117-130.

Toro, E. F. (2001) Shock-capturing methods for free-surface shallow flows, John Wiley, England.

Wu, W., Wang, S., and Jia, Y. (2000) Nonuniform sediment transport in alluvial rivers. *Journal of Hydraulic Research* 38(6): 427-434.

Wu, W. (2007) Computational river dynamics, Taylor & Francis, London.

Xie, J. ed. (1990) River Modelling, China Water and Power Press, Beijing (in Chinese).

Yuan, W., Yin, D., Finlayson, B., and Chen, Z. (2012) Assessing the potential for change in the middle Yangtze River channel following impoundment of the Three Gorges Dam. *Geomorphology*,147-148: 27-34

Zhang, R., and Xie, J. (1993). Sedimentation research in China-systematic selections. Beijing, China: China Water and Power Press (in Chinese).